OFFICE OF NAVAL RESEARCH

Contract N5ori 07841

Project No. NR 031-356

TECHNICAL REPORT NO. 4

September 30, 1953

Metal Processing Division

Department of Metallurgy

Massachusetts Institute of Technology

Cambridge, Massachusetts

OFFICE OF NAVAL RESEARCH

Contract N5ori-07841

Project No. NR 031-356

Technical Report No. 4

September 30, 1953

THE DUCTILE FRACTURE OF METALS

Mechanical Anisotropy in SAE 4340 Steel

by

Davis S. Fields, Jr.

Walter A. Backofen

John Wulff

Metals Processing Division

Department of Metallurgy

Massachusetts Institute of Technology
Cambridge, Massachusetts

DISTRIBUTION LIST

Technical and Summary Reports

<u>Contract N5ori-07841</u>

Chief of Naval Research
Department of the Navy
Washington 25, D. C.
Attn: Code 423 (2)

Commanding Officer
Office of Naval Research
Branch Office
495 Summer Street
Boston 10, Massachusetts (2)

Commanding Officer
Office of Naval Research
Branch Office
50 Church Street
New York 7, New York (1)

Commanding Officer
Office of Naval Research
Branch Office
844 N. Rush Street
Chicago 11, Illinois (1)

Commanding Officer
Office of Naval Research
Branch Office
801 Donahue Street
San Francisco 25, Calif. (1)

Commanding Officer
Office of Naval Research
Branch Office
1030 Green Street
Pasadena, California (1)

Assistant Naval Attache
for Research
London, England
U.S. Navy FPO #100
New York, New York (1)

<u>Project NR 031-356</u>

Director, Naval Research Laboratory
Washington 25, D. C.
Attn: [illegible]. Information Officer (6)

Dr. R. F. Mehl
Carnegie Institute of Technology
Metals Research Laboratory
Schenley Park
Pittsburgh 13, Pennsylvania (1)

Dr. W. M. Baldwin
Case Institute of Technology
Metals Research Laboratory
Cleveland 6, Ohio (1)

Dr. W. C. Craig
Armour Research Foundation
Technology Center
Chicago 16, Illinois (1)

Dr. R. M. Brick
University of Pennsylvania
Philadelphia, Pennsylvania (1)

Dr. Robert Maddin
Johns Hopkins Uni[illegible]
1315 St. Paul [illegible]
Baltimore 2, Maryland (1)

Dr. T. A. Read
Columbia University
New York, New York (1)

Dr. E. P. Klier
University of Maryland
College Park, Maryland (1)

Dr. P. A. Beck
University of Notre Dame
Notre Dame, Indiana (1)

Dr. E. P. Parker
University of California
Berkeley 4, California (1)

NAVY

Director, Naval Research Laboratory
Washington 25, D. C.
Attn: Code 3500, Metallurgy Div.2 (1)
Code 2020, Tech. Library (1)
Code 3800, Mechanics Div. (1)

Bureau of Aeronautics
Department of the Navy
Washington 25, D. C.
Attn: N. E. Promisel, AE-41 (3)
Technical Library, TD-41 (1)

Commanding Officer
Naval Air Materiel Center
Naval Base Station
Philadelphia, Pa.
Attn: Aeronautical Materials Lab. (1)

Bureau of Ordnance
Department of the Navy
Washington 25, D. C.
Attn: Rex (3)
Technical Library, Ad3 (1)

Superintendent, Naval Gun Factory
Washington 20, D. C.
Attn: Metallurgical Lab., IN910 (1)

Commanding Officer
U.S. Naval Ordnance Laboratory
White Oaks, Maryland (1)

Commanding Officer
U.S. Naval Ordnance Test Station
Inyokern, California (1)

Bureau of Ships
Department of the Navy
Washington 25, D.C.
Attn: Code 343 (3)
Code 337L, Tech. Library (1)

U.S. Naval Engineering Experiment Station
Annapolis, Maryland
Attn: Metals Laboratory (1)

Director, Materials Laboratory
Building 291
New York Naval Shipyard
Brooklyn 1, New York
Attn: Code 907 (1)

NAVY

Bureau of Yards and Docks
Department of the Navy
Washington 25, D. C.
Attn: Research & Standards Division (1)

Post Graduate School
U.S. Naval Academy
Annapolis, Maryland
Attn: Dept. of Metallurgy (1)

ARMY

Chief of Staff, U.S. Army
The Pentagon
Washington 25, D. C.
Attn: Director of Research and Development (1)

Office of the Chief of Ordnance
Research and Development Service
Department of the Army
Washington 25, D. C.
Attn: ORDTB (3)

Commanding Officer
Watertown Arsenal
Watertown, Massachusetts
Attn: Laboratory Division (1)

Office of the Chief of Engineers
Department of the Army
Washington 25, D. C.
Attn: Research and Development Branch (1)

AIR FORCE

U. S. Air Force
Research & Development Division
The Pentagon
Washington 25, D. C. (1)

Air Materiel Command
Wright-Patterson Air Force Base
Dayton, Ohio
Attn: Materials Lab.- MCREXM (2)

Office of Air Research
Wright Field
Dayton, Ohio
Attn: Metallurgy Division (1)

DISTRIBUTION LIST - Technical and Summary Reports -- Continued
Contract N5ori-07841 Project NR 031-356

OTHER GOVERNMENT AGENCIES

Atomic Energy Commission
Division of Research
Metallurgical Branch
Washington 25, D. C. (1)

National Bureau of Standards
Washington 25, D. C.
Attn: Physical Metallurgy Div. (1)

National Advisory Committee for
Aeronautics
1724 F Street, N. W.
Washington 25, D. C. (1)

Research and Development Board
Committee on Basic Physical Sciences
The Pentagon
Washington 25, D. C.
Attn: Metallurgy Panel (1)

U. S Atomic Energy Commission
1901 Constitution Ave., N. Y.
Attn: B. M. Fry (2)

Armed Services Technical Information Agency
Documents Service Center
Knott Building
Dayton 2, Ohio (5)

Office of Technical Services
Department of Commerce
Washington 25, D. C. (1)

DISTRIBUTION LIST - Technical and Summary Reports -- Continued
Contract N5 ori-07841 Project NR 031-356

Argonne National Laboratory
P.O. Box 5207
Chicago 80, Illinois
Attn: Dr. Hoylande D. Young (1)

Brookhaven National Laboratory
Information and Publication Division
Documents Section
Uptom, New York
Attn: Miss Mary E. Waisman (1)

Carbide and Carbon Chemicals Div.
Plant Records Dep rtment
Central Files (k- 5)
P.O. Box P
Oak Ridge, Tennessee (1)

Carbide and Carbon Chemicals Div.
Central Reports and Information
Office (-12)
P.O. Box P
Oak Ridge, Tennessee (1)

General Electric Company
Technical Services Division
Technical Information Group
P.O. Box 100
Richland, Washington
Attn: Miss M. G. Freidank (1)

Iowa State College
P.O. Box 14A, Station A
Ames, Iowa
Attn: Dr. F. H. Spedding (1)

Knolls Atomic Power Laboratory
P.O. Box 1072
Schenectady, New York
Attn: Document Librarian (1)

Los Alamos Scientific Laboratory
P. O. Box 1663
Los Alamos, New Mexico
Attn: Document Custodian (1)

Mound Laboratory
U. S. Atomic Energy Commission
P. O. Box 32
Miamisburg, Ohio
Attn: Dr. M. M. Haring (1)

U.S. Atomic Energy Commission
New York Operations Office
P. O. Box 30, Ansonia Station
New York 23, New York
Attn: Div. of Technical Information and Declassification Serv. (1)

Oak Ridge National Laboratory
P. O. Box P
Oak Ridge, Tennessee
Attn: Central Files (1)

Sandia Corporation
Sandia Base
Classified Document Division
Albuquerque, New Mexico
Attn: Mr. Dale N. Evans (1)

U.S. Atomic Energy Commission
Library Branch, Tech. Information
Service, ORE
P.O. Box E
Oak Ridge, Tennessee (1)

University of California
Radiation Laboratory
Information Division
Room 128, Building 50
Berkeley, California
Attn: Dr. R. K. Wakerling (1)

Westinghouse Electric Corporation
Atomic Power Division
P.O. Box 1468
Pittsburgh 30, Pennsylvania
Attn: Librarian (1)

DISTRIBUTION LIST - Technical and Summary Reports -- Continued
Contract N5 ori-07841 Project NR 031-356

Dr. John Dorn
University of California
Berkeley 4, California (1)

Dr. Pol Duwez
California Institute of Technology
Pasadena 4, California (1)

Dr. D. S. Clark
California Institute of Technology
Pasadena 4, California (1)

Dr. N. M. Newmark
University of Illinois
Urbana, Illinois (1)

Dr. T. J. Dolan
University of Illinois
Urbana, Illinois (1)

Dr. H. Eyring
University of Utah
Salt Lake City, Utah (1)

Dr. Finn Johassen
National Academy of Sciences
2101 Constitution Avenue
Washington 25, D. C. (1)

Dr. Max Gensamer
Columbia University
New York, N. Y. (1)

Prof. C. W. Macgregor
University of Pennsylvania
Philadelphia, Pennsylvania (1)

Dr. W. H. Hibbard
General Electric Company
Schenectady, New York (1)

Prof. C. S. Smith
Institute for Study of Metals
University of Chicago
Chicago, Illinois (1)

Prof. Amos J. Shaler
The Pennsylvania State College
State College, Pennsylvania (1)

Dr. J. H. Hollomon
General Electric Company
Schenectady, New York (1)

Dr. P. Coheur
Centre National de Recherches
Metallurgiques
Liege, Belgium
Via: Assistant Naval Attache for
Research
U.S. Navy
FPO 100
New York, N. Y. (1)

Prof. Mott
University of Bristol
Royal Fork
Bristol 8, England
Via: Assistant Naval Attache
for Research
U.S. Navy
FPO 100
New York, N. Y. (1)

Dr. C. F. Tipper
Department of Engineering
Cambridge University, England
Via: Assistant Naval Attache
for Research
U.S. Navy
FPO 100
New York, N. Y. (1)

Prof. E. Orowan
Department of Mechanical Engineering
Mass. Inst. of Technology
Cambridge 39, Massachusetts (1)

Prof. H. W. Swift
Department of Engineering
Sheffield University, England
Via: Assistant Naval Attache
for Research
U.S. Navy
FPO 100
New York, N. Y. (1)

Dr. J. T. Ransom
Materials of Construction Section
E. I. du Pont de Nemours & Co.
Wilmington, Delaware (1)

ABSTRACT

The tensile fracture characteristics after various amounts of torsional prestrain have been studied in specimens of SAE 4340 steel of three grades: vacuum-melted, aircraft quality, and commercial quality. The presence of a submicroscopic crack structure is indicated in all three grades by the transition from high to low values of tensile fracture stress and strain-to-fracture, after critical amounts of prestrain in torsion. The vacuum-melted steel, which is practically inclusion-free, is affected somewhat more by twisting; in particular, the critical prestrain value is lower. The commercial and aircraft grades, however, are practically identical in their response to prestraining. It appears, therefore, that inclusions are not the principal source of microcracks in the materials tested, and that static transverse properties are not greatly influenced by inclusion content, within the range encountered in this work. Since there is a marked difference in grain size between the commercial and aircraft quality steels, it is also concluded that prior austenitic grain size is not a primary factor in the behavior studied. Certain systematic scatter in the data is explained on the basis of oriented microcracks.

INTRODUCTION

The anisotropy in fracture characteristics* of many wrought materials has been studied. Wells, Mehl, and their co-workers,[1,2,3] in particular, have made extensive statistical comparisons of the longitudinal and transverse tensile properties of forged low alloy steel. Figure 1 shows that the reduction in area at fracture varies with the

* Tensile fracture characteristics considered are strain-to-fracture, expressed as a percent reduction in area, and the average true stress at fracture.

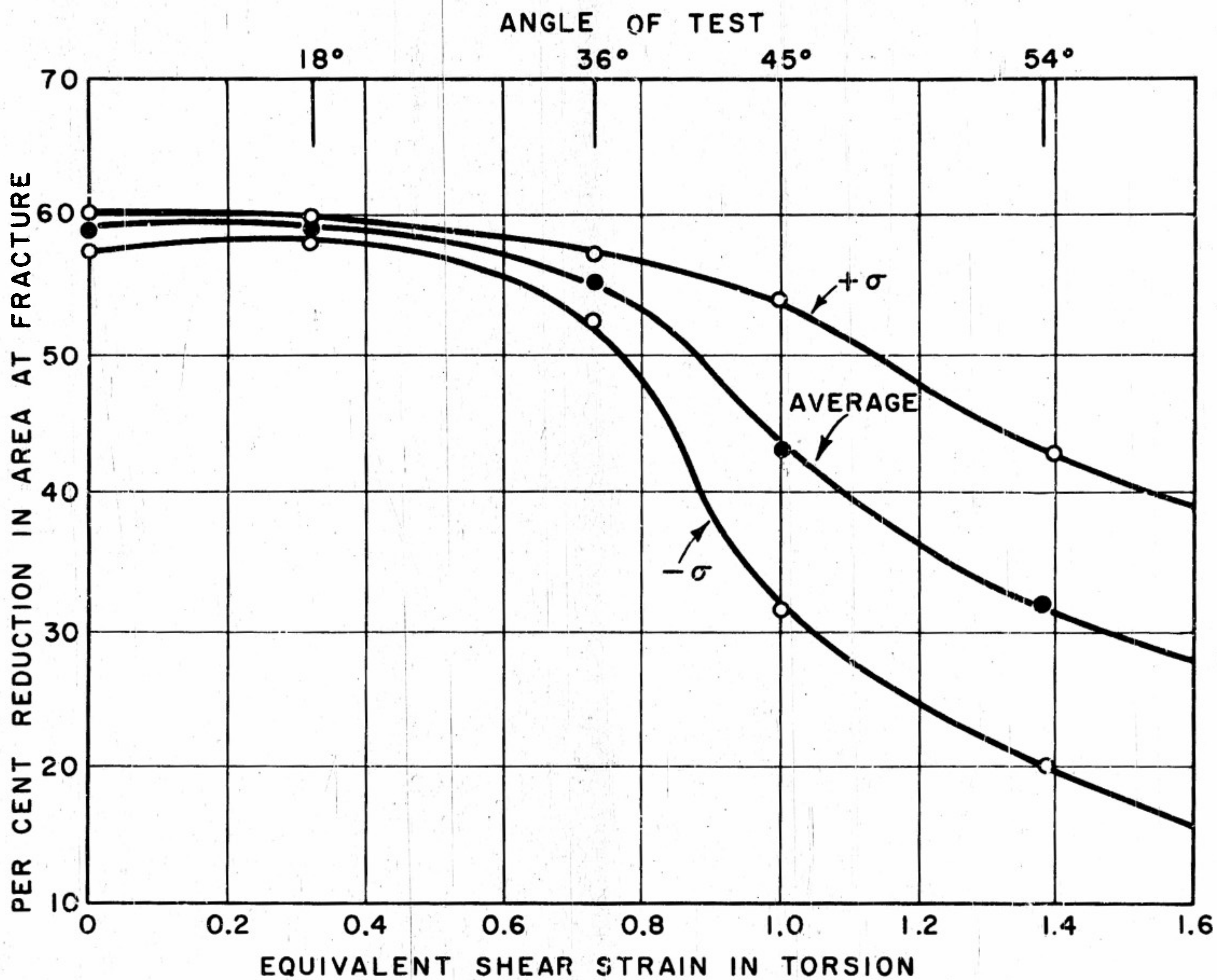

Figure 1

The Effect of Angle of Test upon the Ductility of SAE 1045 Steel (Reconstructed from Grobe, Wells, and Mehl,[3] with an abscissa of "Equivalent Shear Strain": $\gamma = \tan \phi$)

angle of test; it is a maximum in the flow (forging) direction, and a minimum in the transverse direction. Among other workers in this field, Jacquesson and Laurent[4] have observed that the fatigue strength of rolled, high purity aluminum decreases with the angle of test in a somewhat similar manner. The tensile fracture characteristics of hot-rolled plate of the aluminum alloy, 24ST, also have been shown[5] to be greater along and near the rolling direction.

Prompted by the work of Griffith[6] on truly brittle materials, it has been suggested[7] that cracks of submicroscopic size may be present in ductile metals. They would very likely be elongated during plastic deformation, and certainly aligned parallel to the direction of metal flow. Ductility and fracture stress should then be lowest when tension is applied in a direction perpendicular to these cracks.

Swift[8] observed that the fracture characteristics of mild steel tested in tension decrease sharply when specimens are first twisted to a surface shear strain of approximately unity. Simultaneously the ductile, cup-and-cone type of fracture is replaced by a helical, "wolf-eared" one. Specimens twisted and completely untwisted before testing retain their original fracture properties and mode of failure.

Recent work by Backofen and Hundy,[9] and also by Backofen, Shaler, and Hundy,[10] has demonstrated this behavior in OFHC copper, 70-30 brass, nickel, Monel metal, Armco iron, and high purity (99.99%) aluminum. Commercially pure (2S) aluminum was the only material tested which did not

respond to prestraining in the described fashion.

The effect is explained in terms of aligned microcracks. In a bar which has been heavily reduced by rolling, forging, swaging, etc., all of the cracks will be aligned parallel to the direction of elongation. During twisting of a specimen taken parallel to this direction, the cracks will be realigned at an angle ϕ to the specimen axis, so that

$$\tan \phi = \frac{r\theta}{l} = \gamma$$

where r is the distance of the crack from the specimen axis, θ is the total angle of twist in radians, and l is the length of the specimen in which twisting occurs; γ defines the shear strain at the radius r from the specimen axis and it varies linearly from zero at the center to its maximum value at the surface of the bar. In an untwisted bar, ϕ will be zero, and tension on the specimen, before necking occurs, applies no normal stress to the cracks. After a critical amount of twisting, ϕ becomes sufficiently large that stresses acting on the cracks can cause failure through their extension. Untwisting a twisted specimen before testing realigns the cracks parallel to the bar axis where they have a minimum of influence upon fracture characteristics.

It was further observed[9,10] that the angle of fracture in twisted specimens was very close to the calculated angle, ϕ. Neither this observation nor that of the restoration of ductility by untwisting can be suitably explained by theories not based upon aligned defects in the metal.

The nature of microcracks is still unclear. They may be inherent in the casting. On the other hand, in ductile metals they may be generated by the deformation itself;[11,12] brittle phases in the microstructure, such as cementite plates in steel, may be fractured as the ductile matrix-material deforms. A local accumulation of dislocations could be considered to form a microcrack. Yet discontinuities due to nonmetallic inclusions and other extra phases in the microstructure are the only observable "flaws" in otherwise sound metal which might account for the measured anisotropy.

Very striking evidence that inclusions contribute to anisotropy has just been reported by Ransom,[13] who found that the transverse fatigue strength of vacuum-melted, essentially inclusion-free SAE 4340 steel averaged fifty percent higher than the same property of commercial SAE 4340. He showed that fatigue cracks propogate from the edges of elongated inclusions when they are acted upon either by a principal tensile stress or a maximum shear stress. However, even in the vacuum-melted steel the ratio of transverse to longitudinal fatigue strength was only 0.86. This shows that even when the inclusion content is practically nil, there is still a fibrous structure producing anisotropic properties. Banding was a problem in the ultra-clean steel, and might contribute to this fatigue strength ratio of less than one; but the contribution from a highly oriented crack structure has not been ruled out.

In the past, much consideration has been given to the possibility

of controlling transverse properties in wrought steel through control of the size, shape, and distribution of non-metallic inclusions. The presence of a highly oriented crack structure suggests that there might be a limit to what can be accomplished with such control. Therefore it was the purpose of this research to determine the tensile fracture characteristics of SAE 4340 steel of three degrees of cleanliness after prestraining in torsion; and, in this way, to study relationships between anisotropy in fracture characteristics, the crack structure, and inclusion content.

EXPERIMENTAL PROCEDURES

Materials and Processing

Chemical analyses of the three steels tested are summarized in Table I. Those of aircraft and commercial quality were from regular heats of SAE 4340 steel. The vacuum-melted sample was from an experimental heat described by Ransom.[13] It varies from the nominal SAE 4340 composition principally in the absence of phosphorous, sulphur, and retained gases.

TABLE I

Analyses of Steels (Percent by Weight)

	Vacuum-Melted	Aircraft Quality	Commercial Quality
Carbon	0.39	0.41	0.41
Manganese	0.69	0.75	0.80
Phosphorous	nil	0.009	0.033
Sulphur	nil	0.014	0.019
Silicon	0.37	0.31	0.28
Nickel	1.78	1.79	1.72
Chromium	0.97	0.84	0.82
Molybdenum	0.31	0.26	0.24
Vanadium	0.13	nil	nil
Nitrogen	2.5×10^{-4}	6×10^{-3}*	6×10^{-3}*
Oxygen	1.8×10^{-3}	8×10^{-3}*	8×10^{-3}*
Producer	National Research Corp.	United States Steel Corp.	United States Steel Corp.
Heat No.	....	9X5510	9X5778

*Nominal values from ASM Metals Handbook

Materials were received from suppliers as two and one-half inch diameter, hot-forged rounds approximately one foot long. Each sample was hot-swaged above 1800°F to seven-eighths inch diameter. The bars were then cut into blanks two and one-half inches long, and the vacuum-melted samples were subjected to a twenty-four hour homogenizing treatment at 1900°F. Subsequently all specimens were heat treated by normalizing one hour at 1700°F, austenitizing two hours at 1600°F, oil quenching, tempering four hours at 1200°F, water quenching, re-tempering two hours at 1200°F, and water quenching. The vacuum-melted steel was quite sluggish in its response to tempering; it was necessary to re-temper many of these specimens,

and also a few from the other lots, for additional periods at 1200°F in order to bring their hardnesses down to a common level.

The heat-treated blanks were machined into torsion specimens. Following two-hour stress relief anneals at 1080°F before and after finish machining, they were polished through 0000 emery paper. Specimens were then twisted, machined for tension testing, and again polished through 0000 emery. Dimensions of test bars are shown in Figure 2.

Testing Procedures

The bars were twisted in a torsion testing machine operating at a constant angular speed of ninety degrees per minute. Autographic records of torque versus angle of twist were obtained for all specimens. The shear strain at the surface of the tensile specimen was calculated for each bar.

Tension testing was performed on a hydraulic machine operating in a load range from zero to ten thousand pounds. Values of load and instantaneous minimum bar diameter were determined at frequent intervals during each test. From these readings, a curve of average true stress versus true strain* could be calculated for each specimen. A single test

---

* Definitions of terms:

True stress - the instantaneous load divided by the instantaneous minimum specimen diameter.

True strain - $2 \ln_e(d_o/d)$, where d_o is the original and d the instantaneous specimen diameter.

Engineering tensile strength - the maximum load divided by the original area of the specimen.

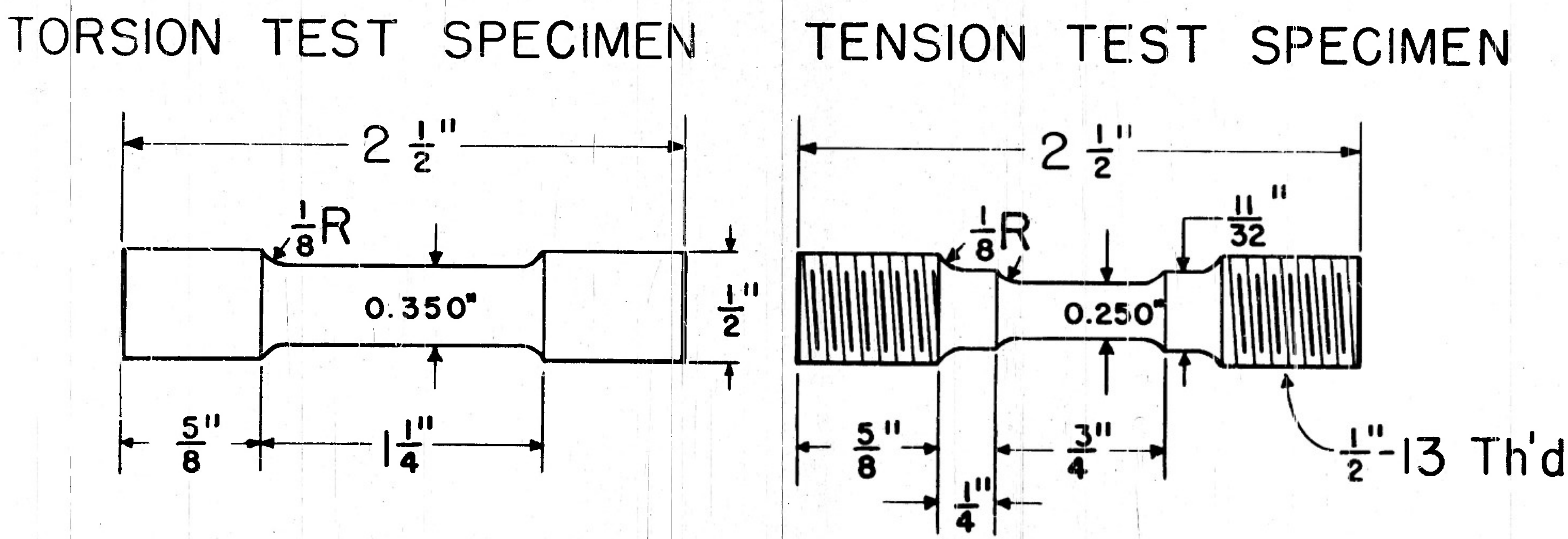

Figure 2

Dimensions of Test Specimens

required approximately twenty minutes to perform. Strain rates were sufficiently low that accurate values of fracture stress, maximum reduction in area, and engineering tensile strength could be determined.

To measure the angles of fracture in specimens failing across helical surfaces, a light circumferential scratch, normal to the specimen axis, was inscribed around the broken specimen just below the point where fracture originated. The angle between this line and the fracture surface was measured with a toolmaker's microscope.

RESULTS OF EXPERIMENTAL WORK

Uniformity of Materials

Every effort was made to insure that the steels would be identical in every respect except inclusion content. Their histories were essentially identical from forged bars to broken specimens. The following observations serve to check the degree to which their properties coincide:

Microstructure: Microstructures of the three steels, at high magnifications, are shown in Figure 3; they all consist of tempered martensite in the spheroidized condition. In addition, the vacuum-melted steel contains a small amount (less than ten percent) of tempered bainite, only partially spheroidized. The photomicrographs of Figure 4 were etched to show the prior austenitic grain size. The vacuum-melted steel has mixed grains, with a majority of ASTM Grain Size No. 2. The aircraft and commercial quality steels are more regular, having ASTM Grain Sizes No. 5 and 10 respectively.

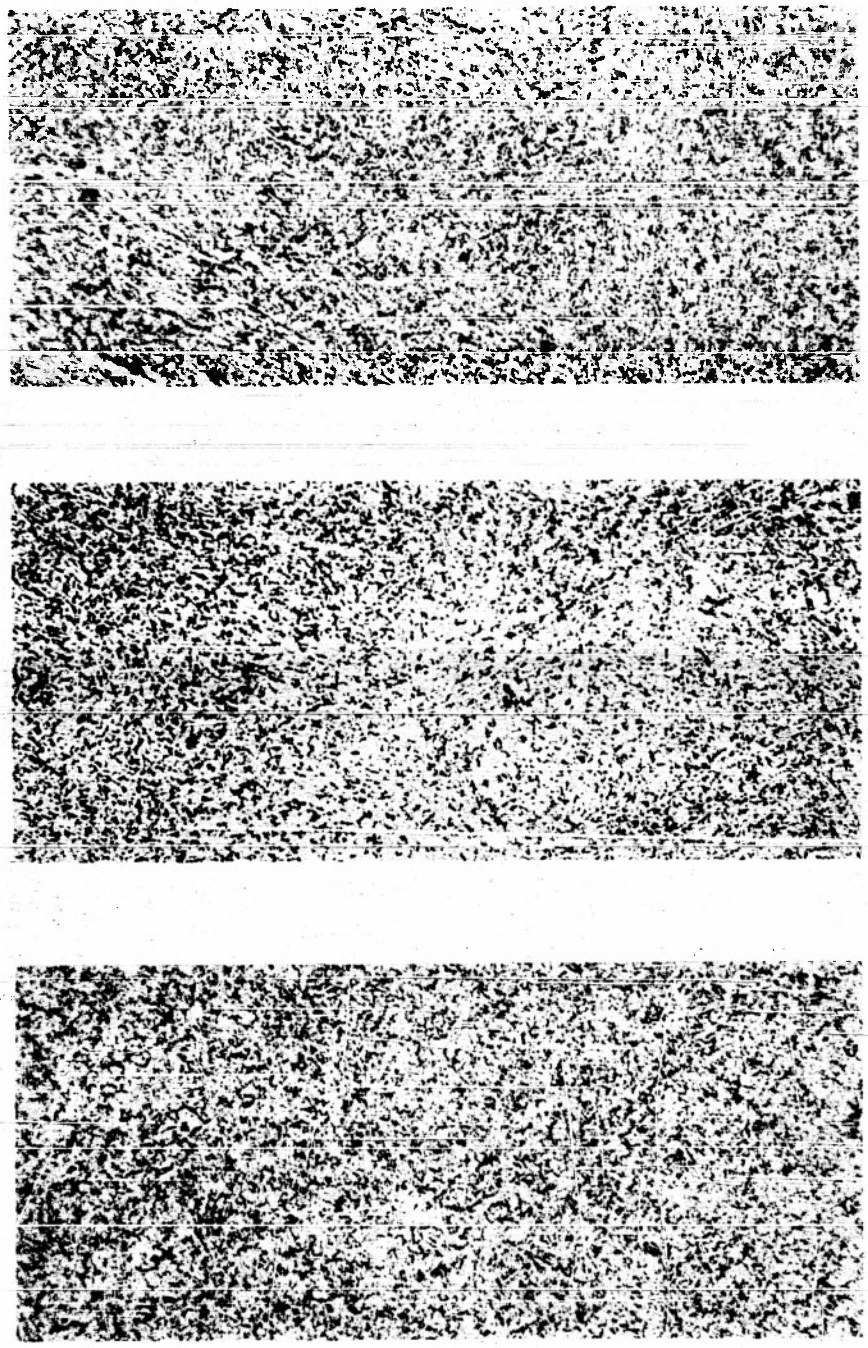

Figure 3

Microstructures of SAE 4340 Steels: (top to bottom) Vacuum-melted, Aircraft Quality, Commercial Quality; Picral Etch

x500

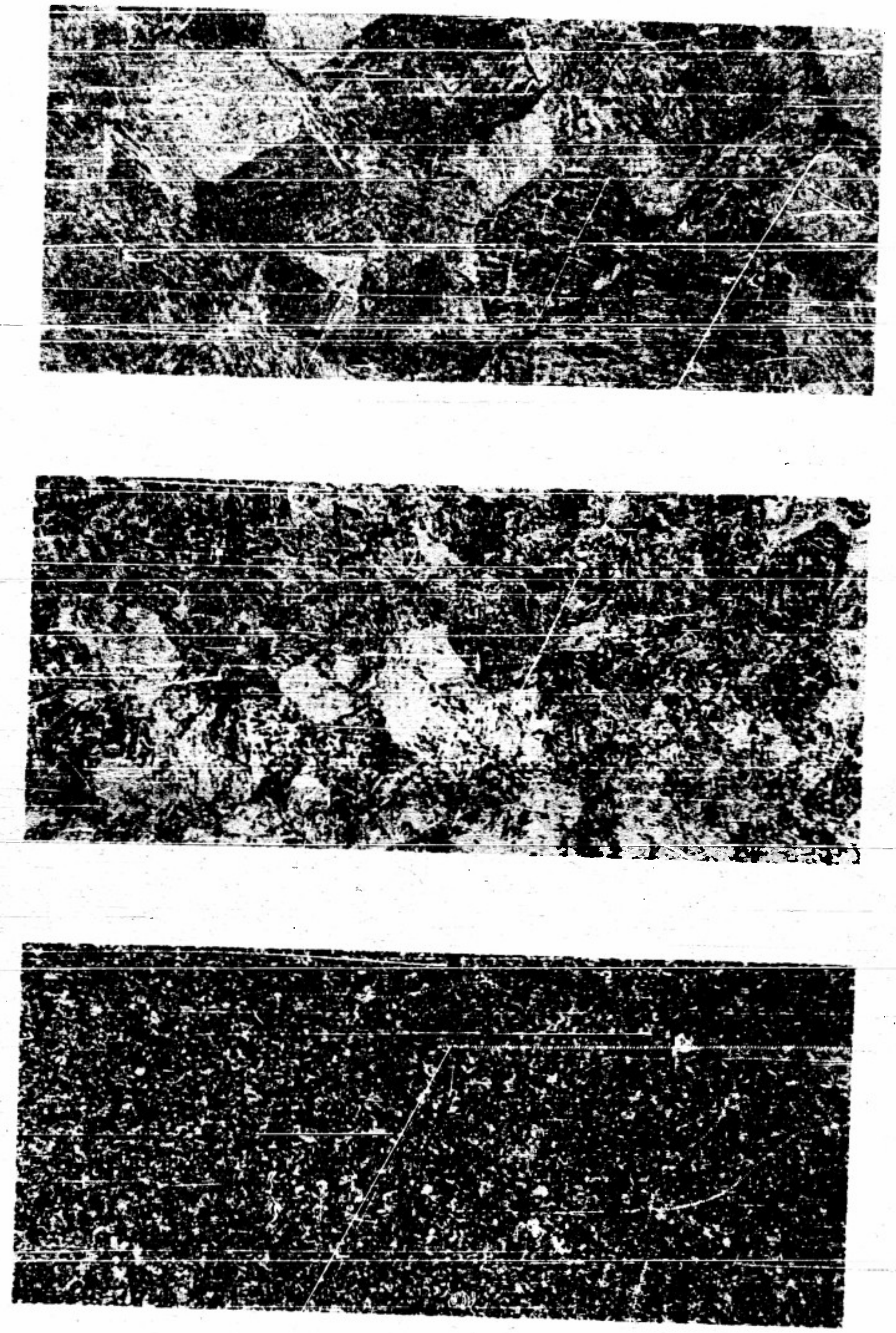

Figure 4

Austenitic Grain Sizes of SAE 4340 Steels: (top to bottom) Vacuum-melted, Aircraft Quality, Commercial Quality; Vilella Etch.

x100

Tension and Torsion Tests: Figure 5 presents typical true stress-true strain curves for untwisted bars tested in tension. The strength levels at a given strain and the strain hardening characteristics are quite similar for the three steels. There is a small, reproducible variation in the reductions-in-area at fracture. For the aircraft quality steel it was sixty-four percent; for the other two, approximately sixty percent.

Figure 6 shows typical torque-twist curves recorded autographically during prestraining. The characteristics of the three steels are almost identical in torsion. The only difference to be noted is the presence of a slight yield point effect in the commercial steel, a less pronounced one in the aircraft quality, and none at all in the vacuum-melted material.

In the "soft" hydraulic machine used for tension testing it was impossible to observe any yield point effects.

Hardness: Heat treatment of the specimens was designed to produce maximum ductility and minimum hardness. Several Rockwell hardness measurements were made on the ground end of each specimen after final heat treatment. The average values for all bars are recorded in Table II.

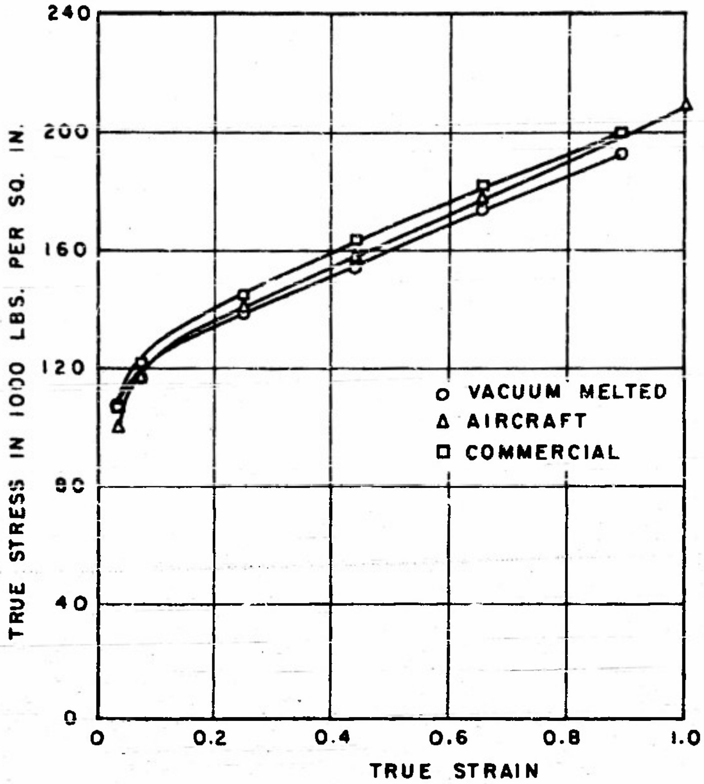

Figure 5

Typical True Stress-True Strain Curves
in Tension for Untwisted Specimens

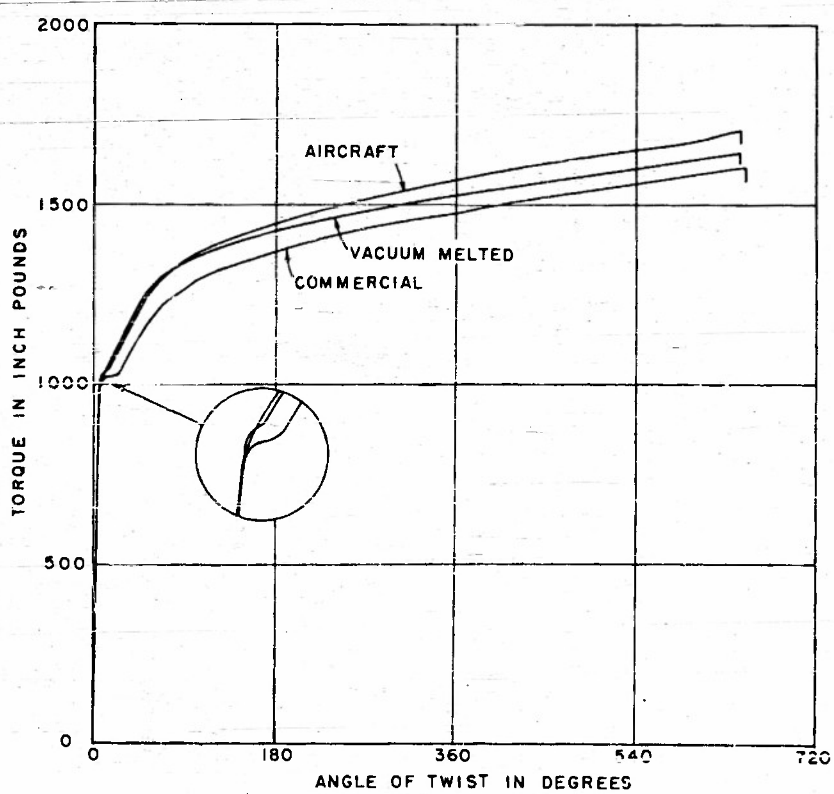

Figure 6

Typical Curves of Torque Versus
Angle of Twist

Table II

Hardness of Specimens

	Mean Hardness Rockwell "C"	Average Deviation from the Mean
Vacuum-melted	15-1/2	1
Aircraft Quality	14-1/2	1
Commercial Quality	19-1/2	1

Inclusion Content: All three of the steels are "clean" by commercial standards. The aircraft and commercial grades have approximately the same density of non-metallic inclusions, with a slight tendency for some to be elongated in the forging direction. The vacuum-melted steel has only the smallest of inclusions; all of them are spherical.

Effect of Torsional Prestrain upon Tensile Properties

The effects of prior twisting upon the tensile fracture characteristics of the vacuum-melted, aircraft quality, and commercial quality steels are shown in Figures 7, 8, and 9, respectively. All of the test points are included with those curves. The specimens supported a sizeable fraction of their maximum loads even after helical cracks were visible in their surfaces. Consequently the curves of average true stress versus true strain in some cases showed a range of strain over which stress remained essentially constant. In this range, elongation occurred both by plastic deformation and by propagation of the cracks. Fracture stress and reduction in area values at fracture were chosen as the points at which the

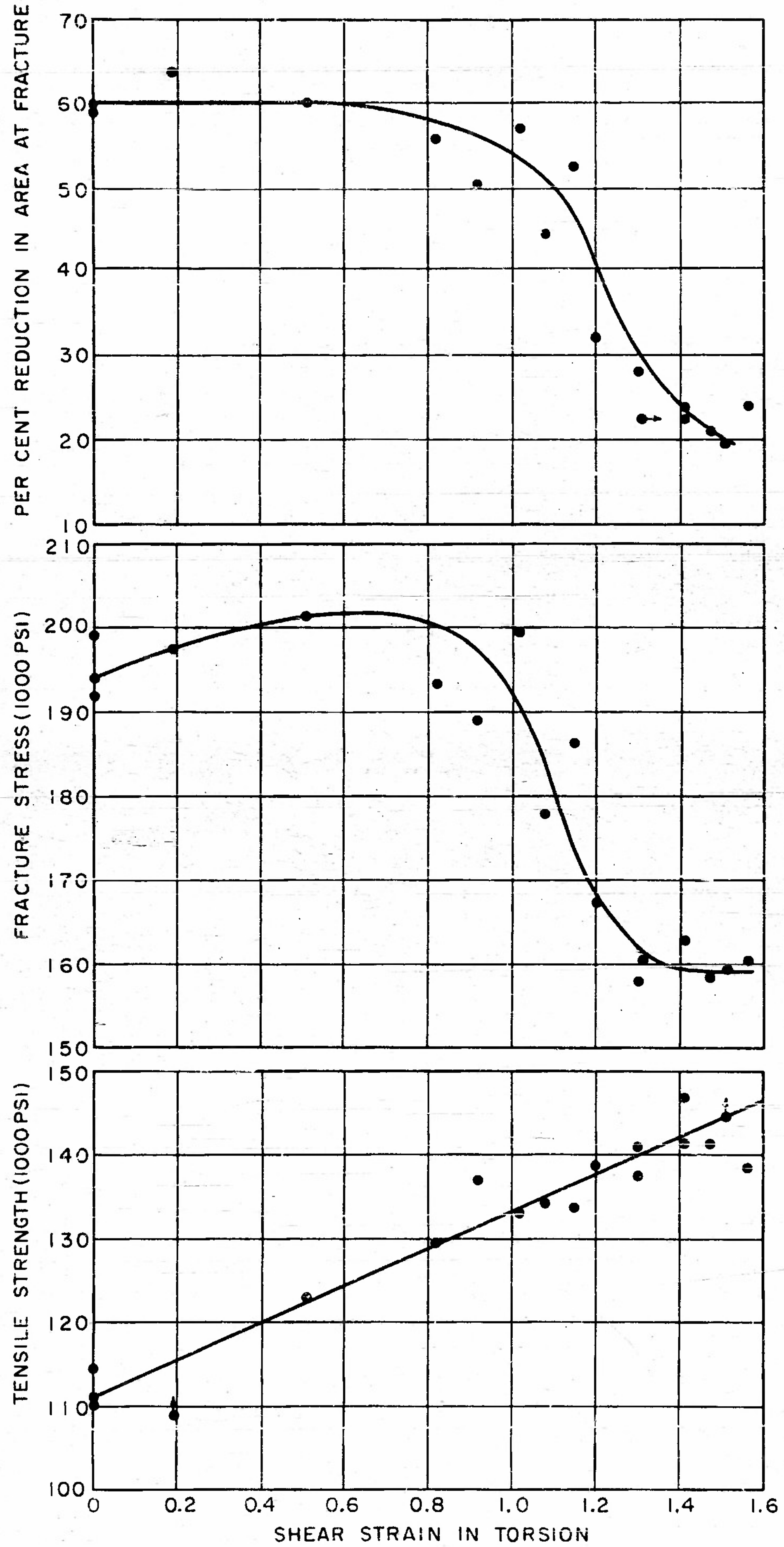

Figure 7

Effects of Torsional Prestrain upon the Tensile Fracture Characteristics and Tensile Strength of Vacuum-melted SAE 4340 Steel

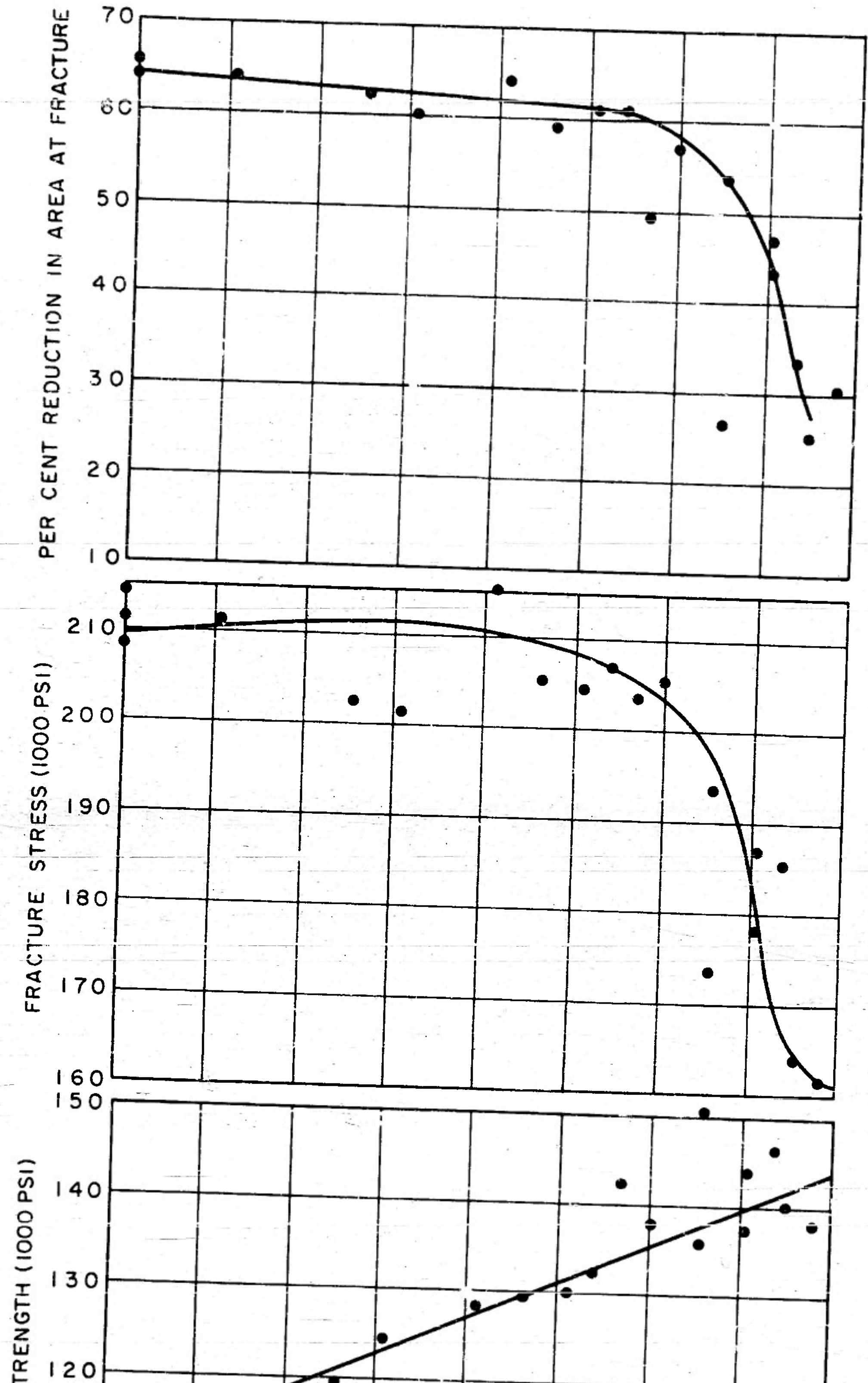

Figure 8

Effects of Torsional Prestrain upon the Tensile Fracture Characteristics and Tensile Strength of Aircraft Quality SAE 4340 Steel

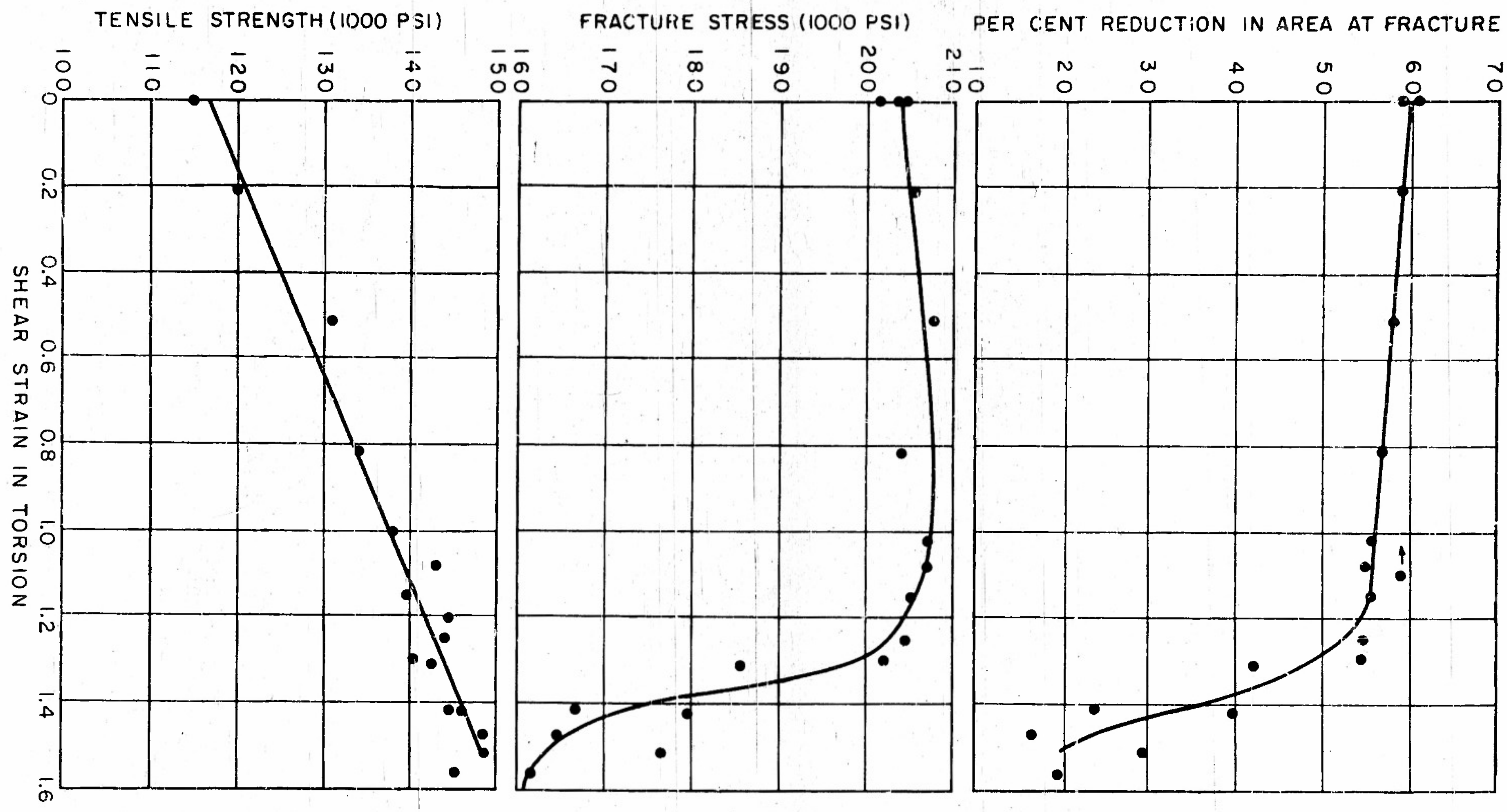

Figure 9

Effects of Torsional Prestrain upon the Tensile Fracture Characteristics and Tensile Strength of Commercial Quality SAE 4340 Steel

true stress-true strain curves deviated from their essentially linear character.

There is considerable scatter in the data. The curves of engineering tensile strength versus prestrain were plotted as an aid in detecting specimens with atypical strengths which might cause anomalous fracture characteristics.

All three steels show an abrupt transition from high to low values of ductility and fracture stress after critical amounts of prior twisting. There was little change in either of these properties as specimens were twisted to surface shear strains of approximately one. At that point, the curves drop sharply. Simultaneously the mode of fracture changes from the cup-and-cone type to an angular or helical one. At the maximum shear strain which could be introduced into the specimens without risking failure in torsion, the curves showed only a slight tendency to approach a constant lower value of either fracture stress or ductility.

Figure 10 superimposes the fracture characteristic and tensile strength curves of the three materials for comparison. The tensile strength values are consistent with the hardness levels of Table II, i.e., the harder materials possess the higher tensile strengths. The levels of fracture stress before transition also reflect this difference, the lowest tensile strength, for example, being associated with the material of highest fracture stress.

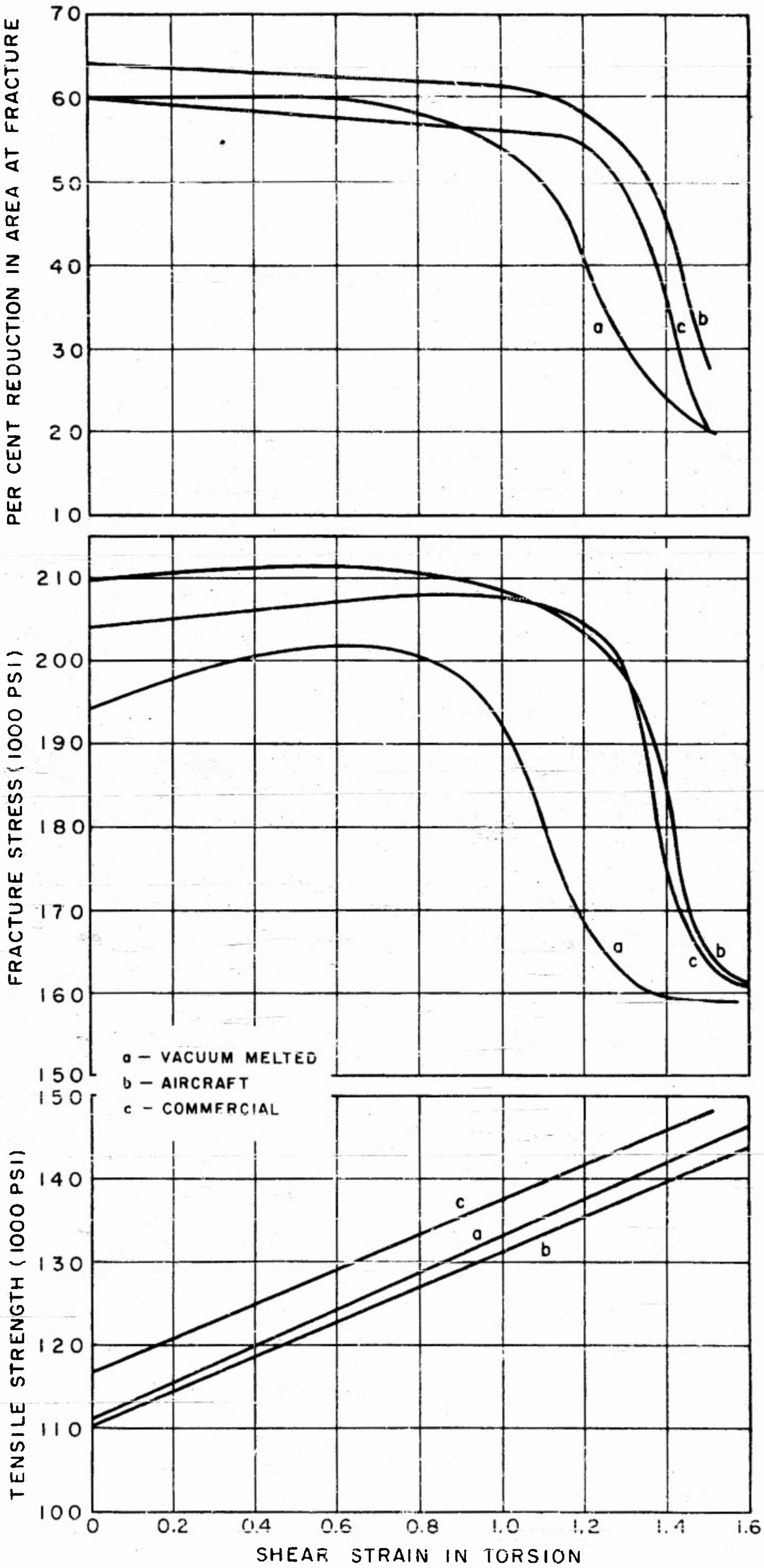

<u>Figure 10</u>

Effects of Torsional Prestrain upon the Tensile Fracture Characteristics and Tensile Strengths of Three Grades of SAE 4340 Steel

The critical shear strain is approximately the same for the aircraft and commercial qualities of steel, and the slopes of the curves in the region of transition are nearly equal. On the other hand, the fracture stress and ductility of the vacuum-melted material begin to fail at a lower prestrain; and the transition is not so sharp.

There was no obvious difference between the fracture surfaces of specimens of different quality but having approximately the same fracture strength and ductility. Before transition, fractures were of the cup-and-cone type originating at the center of the necked specimen. Late in transition, fractures were completely helical or angular. They originated in the highly strained specimen surface, and propogated inward. Between the two extremes there was a compromise fracture exhibiting tendencies towards both types of failure. Cracks evidently propogate both inward and outward in such a case. Figure 11 shows typical fractures in specimens twisted to different amounts of prestrain.

No trend was apparent in the angle-of-fracture versus prestrain data since the range of prestrain was relatively low. The angles were, however, close to those of other materials subjected to the same amount of prior twisting,[9,10] i. e., somewhat larger than the calculated angle at which microcracks would be aligned by twisting. Presumably this is due to rotation of the microcracks back toward the specimen axis during deformation prior to fracture during testing.

Figure 11

Tensile Fractures of Specimens Previously Prestrained in Torsion: (left to right, γ = 0, 1.15, 1.48, and 1.50). Approximately twice actual size.

DISCUSSION OF EXPERIMENTAL RESULTS

As Figure 10 shows, the tensile fracture characteristics of each of the three grades of SAE 4340 steel are influenced approximately the same way by torsional prestraining. Interpretation of the data requires the presence of a highly oriented crack structure initially aligned in the direction of the specimen axis.[9,10] Torsion-tension testing and conventional testing to establish the relationship between longitudinal and transverse properties (Figure 1) are similar; therefore information from the one kind of testing should be similar to that produced by the other.

The similarity of the results for the three steels is rather surprising inasmuch as they differed in several respects: cleanliness, prior austenitic grain size, and chemical composition. A further but probably insignificant microstructural difference of about ten percent partially spheroidized bainite existed between the vacuum-melted and the other two grades.

It would be expected that inclusions in the steel, especially those aligned normal to the testing direction, would provide points of weakness at which failure could begin. Indeed, in fatigue testing in the transverse direction, cracks do propogate from the ends of elongated inclusions.[13] However, over the range of inclusion contents studied- and these are admittedly "clean" steels- they have no significant effect upon the anisotropy of the statically determined fracture characteristics. The cleanest steel is, in fact, the most highly anisotropic; and one cannot

possibly consider this to be due to the absence of inclusions. The results, then, must be the consequence of a highly oriented crack structure in all steels. Whereas a transverse fatigue failure occurs after local damage near the few largest cracks (inclusions) in the specimen, failure in static testing is not so localized, and must be due to the simultaneous growth of many microcracks whose density in the specimens is very high.

A question that still must be answered is why the vacuum-melted steel has the greater sensitivity to prestraining. The large prior austenitic grain size (Figure 4) can be discounted as the only cause, since the commercial and aircraft quality steels have identical fracture characteristics while exhibiting a pronounced difference in grain size. The variations in chemical composition and in microstructure, except for grain size, are slight; flow characteristics (Figures 5 and 6) are hardly affected by them, and it seems logical to draw the same conclusion about the fracture characteristics. Ransom[13] reported that the vacuum-melted steel had pronounced longitudinal banding as 2-1/2 inch round stock. After the additional swaging and homogenization heat treatment used in the present research, only the slightest banding was observable; again it seems hardly likely that the variable is a significant one.

The unusual processing history of the ultra-clean steel probably is most likely responsible for its lower critical shear strain. Both the special melting practice and the lower amounts of reduction given to the small cast ingot could have some bearing upon the nature of the crack structure.

Scatter in data

Figure 1 shows not only the variation of reduction in area with the angle of test in a forged steel, but also the standard deviations of the data. It plots the data of Grobe, Wells, and Mehl[3] in terms of equivalent torsional shear strain, where the equivalent strain is simply the tangent of the angle between the test specimen axis and the flow direction. For any particular crack orientation represented in Figure 1, a shear strain equal to the corresponding equivalent amount would be required to provide this orientation if initially the cracks were aligned parallel to the specimen axis.

A significant part of the data in Figure 1, which is reflected in the scatter of points in Figures 7, 8, and 9, is the variation of the standard deviation with the angle of test; this has an explanation in terms of microcracks. As the crack structure becomes inclined at larger angles to the specimen axis, either through prestraining or selection of test specimens, it exerts a greater influence on fracture characteristics. The size of the largest crack in the considerably dense structure that must exist -- the one that initiates the angular or helical fracture -- will vary in a statistical manner from specimen to specimen. Since the stress required for fracture must be some inverse function of the crack length, it is reasonable to believe that the variation in crack size can cause large scatter in fracture characteristics in or near the transverse direction. Near the longitudinal direction, the cracks play a less active role in

fracture, and the data suffer much less variation.

Inhomogeneous yielding

Figure 6 shows that inhomogeneous yielding during torsion testing is most pronounced in the commercial quality steel, is somewhat less in the aircraft quality, and is absent in the vacuum-melted grade. Such yielding in steel has been attributed to interstitially dissolved carbon and nitrogen. However, the carbon contents of the three grades are practically the same, while there is at least a ten-fold variation in nitrogen content. Since the yielding occurs only in the high-nitrogen steels, this element might be held responsible for it.

One important variable which must be accounted for is grain size. The yield-point effect in tensile deformation is known to increase with decreasing grain size. Since that steel showing the most pronounced effect in the present work also has the smallest grain size, it may be that this variable is the significant one. The roles of chemistry and grain size cannot be separated in this instance; they are very likely making a joint contribution.

SUMMARY AND CONCLUSIONS

Forged SAE 4340 steel of three different grades, vacuum-melted, aircraft quality, and commercial quality, like most pure metals and single phase alloys, contains a structure of submicroscopic, crack-like defects which are aligned parallel to the flow direction of the wrought material.

This leads to marked anisotropy of tensile fracture characteristics, as determined by tension testing after prestraining in torsion. The density of these microcracks is apparently unrelated to inclusion content, and therefore it appears that anisotropy cannot be entirely eliminated even by resorting to ultra-clean steels.

ACKNOWLEDGMENTS

The authors are indebted to the Office of Naval Research for sponsoring this research program, and to Dr. J. T. Ransom of E.I. duPont de Nemours & Co. for kindly providing the vacuum-melted steel.

REFERENCES

1. Wells, C., and Mehl, R. F.: Trans. A.S.M., 41 (1949), p. 717

2. Olds, E. G., and Wells, C.: Trans. A.S.M., 42 (1950), p. 845

3. Grobe, A. H., Wells, C., and Mehl, R. F.: Trans. A.S.M., 45 (1953), p. 1080

4. Jacquesson, R. and Laurent, P.: Revue de Metallurgie, (1949), p. 89. Abstract in Metal Progress, 59 (1951). p. 422.

5. Klinger, L. J. and Sachs, G.: Jour. of the Aero. Sciences, 15 (1948), p. 731

6. Griffith, A.: Phil. Trans. Roy. Soc., 221 (1920), p. 163, and Proc. Int. Cong. App. Mech. (1924), p. 55

7. Hollomon, J. H.: The Problem of Fracture, American Welding Society (1946)

8. Swift, J. H.: Jour. of the Iron and Steel Inst., 140 (1939), p. 181

9. Backofen, W. A. and Hundy, B. B.: Jour. of the Inst. of Metals, 81 (1953), p. 443

10. Backofen, W. A., Shaler, A. J., and Hundy, B. B.: Trans. A.S.M., 46 (1954), to be published.

11. Zener, C. and Hollomon, J. H.: Trans. A.S.M., 33, (1944), p. 163

12. Zener, C.: Fracturing of Metals, American Society for Metals (1947), p. 3

13. Ransom, J. T.: Trans. A.S.M., 46 (1954), to be published.